Strain and Acceleration-Based Finite Element Model Updating of a Concrete Highway Viaduct

DORON HEKIC, ANDREJ ANZLIN, DIOGO RIBEIRO, ALES ZNIDARIC and PETER CESAREK

SUMMARY

This paper presents a finite element model updating (FEMU) study performed on a single span of a multi-span concrete highway viaduct, equipped with permanent monitoring and a bridge weigh-in-motion (B-WIM) system. The paper focuses on the comparison of updated variables from two different types of measurements: (1) longitudinal strains, induced by calibration vehicles and measured by sensors primarily used for B-WIM, and (2) natural frequencies of the superstructure, that were obtained from ambient and traffic-induced vibrations. In addition, the contribution of the concrete safety barriers to the superstructure stiffness is discussed.

INTRODUCTION

Structural Health Monitoring (SHM) plays a critical role in the lifecycle management of bridges, particularly the older and damaged ones, providing the essential data needed to assess their current state, detect potential failures, and guide maintenance efforts. The primary objective of SHM is the real-time or periodic recording and analysis of various structural responses, such as strain and acceleration, under different loading conditions. Data collected through SHM systems offer a rich source of information that helps engineers better understand the behavior and performance of a bridge, including identifying abnormal trends or anomalies that may signify damage or degrade the structure or demonstrate its suspicious behavior.

Doron Hekič, University of Ljubljana, Faculty of Civil and Geodetic Engineering, 2 Jamova cesta, Ljubljana 1000, Slovenia; Slovenian National Building and Civil Engineering Institute, 12 Dimičeva ulica, Ljubljana 1000, Slovenia
Andrej Anžlin, Slovenian National Building and Civil Engineering Institute, 12 Dimičeva ulica, Ljubljana 1000, Slovenia
Diogo Ribeiro, CONSTRUCT-LESE, School of Engineering, Polytechnic of Porto, Porto 4200-465, Portugal
Aleš Žnidarič, Slovenian National Building and Civil Engineering Institute, 12 Dimičeva ulica, Ljubljana 1000, Slovenia
Peter Češarek, University of Ljubljana, Faculty of Civil and Geodetic Engineering, 2 Jamova cesta, Ljubljana 1000, Slovenia

Maintaining the desired performance of bridges has become increasingly challenging due to the ageing of traffic infrastructure [1] and the projected increase in passenger and freight traffic by over 230% from 2015 to 2050 [2] in OECD countries. Therefore, there is an urgent need for developing and implementing innovative methods and technologies to enable infrastructure managers to monitor the condition of their assets effectively. One potential method for monitoring instrumented structures throughout their life is using Bridge Weigh-in-Motion (B-WIM) systems ([3], [4], [5]) beyond their primary weighing function ([6], [7]) to update the Finite Element (FE) model. This approach extends B-WIM applications and facilitates the use of SHM for short and medium-span bridges.

Structural Health Monitoring (SHM) of Bridges

Traditionally, visual inspections have been used to detect defects and assess structural conditions, but they are subjective, time-consuming and inappropriate for real-time monitoring. SHM has emerged as a promising solution for assessing the condition of civil infrastructures.

SHM involves monitoring structures with sensors, extracting damage features and analyzing them to evaluate structural conditions. For the (continuous) condition assessment of bridges, an updated finite element (FE) model of the bridge is often used to gain insight into structures' property changes, such as stiffness degradation, prestressing losses, scour etc., causing the bridge to deviate in its behavior.

Wang et al. [8] describe a two-phase model updating approach to develop a baseline model for the Runyang suspension bridge in China. The model updating was performed for specific construction phases and after the completion of the bridge. The updating procedure involved modifying the design variables to match the modal parameters (natural frequencies, damping ratios and mode shapes) and static responses (displacements and stresses). The calibrated FE model proved to have a good correlation with the static and dynamic measurements and was used for the continuous condition assessment of the bridge, particularly for damage identification.

Meixedo et al. [9] present a progressive numerical model validation of a bowstring-arch railway bridge located in Alcácer do Sal (Portugal), based on the analysis of experimental data from different structural response measurements, namely, static deformations under environmental actions, modal responses (natural frequencies and mode shapes), and transient dynamic responses under traffic loads. For model validation, reproducing the non-linear behavior at the bearing devices, particularly under slow and traffic actions, was crucial for the very good agreement between experimental and numerical data.

Ereiz et al. [10] provide general guidelines about using SHM data to perform the finite element model updating (FEMU) accurately. The process of model updating is described step by step, namely: 1) selection of updating parameters (design variables), 2) definition of the model updating problem, and 3) solution of the model updating problem using different methods, particularly sensitivity-based, maximum likelihood, non-probabilistic, probabilistic, response surface, meta heuristic, and regularization methods.

Bridge Weigh-in-Motion (B-WIM)

Bridge-WIM or B-WIM refers to a specific method that uses an instrumented bridge or culvert to weigh heavy vehicles while they cross the structure. B-WIM systems provide an equivalent set of vehicle parameters (axle loads, gross weight, axle spacing, velocity, vehicle category…) as the more established pavement WIM systems, but also have some specific advantages:

- The portable hardware, including the sensors, can be installed on and detached from a bridge. Unlike the pavement WIM systems, portable installations provide similar quality results as the permanent ones.
- As the weighing platform, a bridge span is far longer than the width of the sensor built into a road surface, the accuracy of results is generally high, especially on smooth pavements. Installations are also possible on rougher or rutted surfaces, where pavement WIM installations are not even considered.
- In most installations, all sensors are mounted underneath the bridge deck. Consequently, installation and maintenance activities do not interrupt the traffic. This is advantageous for sites where cutting into the pavement is not allowed, or installing a pavement-based system is not feasible due to heavy traffic or where permits for road closures are difficult to obtain.
- Bridges often cannot be avoided, which is not valid for pavement WIM sensors, which generally do not cover the entire road surface width.
- Collected strain records can be used to generate above mentioned indicators (influence lines, dynamic amplification factors, load distribution factors) to monitor bridge performance under traffic loading and thus to optimize bridge assessments ([7], [11]).

It has been shown through theoretical [7] and practical studies [12] that analyses based on B-WIM-based performance indicators can optimize the bridge assessments, particularly at the serviceability limit states. Typical examples are when structural safety has to be determined for the current level of traffic loading, i.e., when a decision is needed on whether a bridge requires some actions. It has been demonstrated that just knowing the true performance of a bridge by measuring the influence lines or its dynamic behavior under traffic loading can drastically reduce the conservatism of the applied analytical methods, which, consequently, results in far less restrictive and costly rehabilitation measures.

MEASUREMENTS

Case Study Viaduct

The case study viaduct located in Slovenia, on the heavily trafficked 5th Trans-European corridor from Venice in Italy to Lviv in Ukraine, is a typical highway viaduct from the 1970s, made of prefabricated prestressed concrete main girders and a cast-in-place slab placed on octagonal cross-section-shaped piers. The two parallel structures are 588 m and 544 m long. The left structure in Figure 1, discussed in this paper, has 17 spans and carries two lanes of traffic from the capital Ljubljana in the western direction towards the border with Italy.

Figure 1. Case study viaduct: View from below (left) and view from above (right).

The harsh environment, the significant amounts of de-icing salt, and the large traffic demand contributed to accelerated degradation and resulted in four major repairs after its completion. Within the last rehabilitation between 2017 and 2019, more than 200 sensors were installed to measure selected structural elements permanently. The setup included a B-WIM system, which uses the data from longitudinal strain measurements on the main girders in the most heavily instrumented span. A one-span FE model extracted from the full FE model was updated in the present study.

Processing of the Measurements

STRAINS AT THE MAIN GIRDERS

B-WIM system is calibrated prior to its operation with calibration vehicles of known axle loads. Data from calibration vehicle passage was used in this study for strain-based FEMU. Figure 2 shows the transverse position of the calibration vehicle on the viaduct and strain gauges mounted near the mid-span of the main girder with a typical time-domain signal caused by the calibration vehicle.

As the entire procedure of the signal processing and methodology to determine the average maximum measured strains for all sensors and calibration vehicle passages is beyond the scope of this paper, an interested reader is referred to [13] for details.

Generally, 51 passages of three different calibration vehicles on the driving lane were considered. The response was measured with 11 strain-gauge sensors installed near the mid-span of 4 main girders (two or three sensors per girder). For each passage and for each sensor, maximum values from the filtered response (Figure 2) were determined as a basis to which modelled strains were compared (updated).

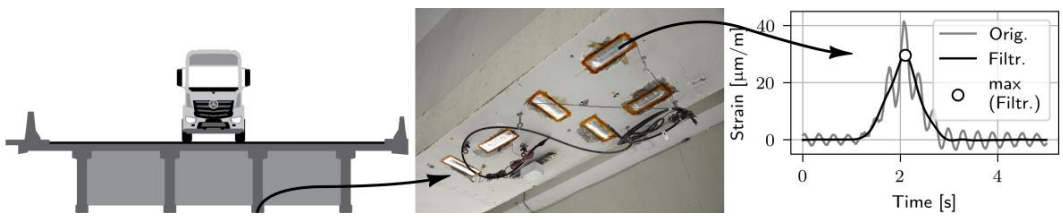

Figure 2. The transverse position of the calibration vehicle (left), strain-gauge sensors for measuring longitudinal strains at main girders (middle) and typical strain response under full-speed calibration vehicle (right).

ACCELERATIONS OF THE MAIN GIRDERS

A separate experimental campaign was performed on the viaduct to measure the accelerations of the superstructure to obtain the modal parameters. Acceleration sensors were distributed over the four spans, covering one entire braking unit (the section between two expansion joints) of the left structure (according to Figure 1), consisting of four overall braking units. Part of this unit is also the most heavily instrumented span, installed with a B-WIM system. Disposition of the 12 reference and mobile sensors was designed such that 40 measurement points covered the entire unit, i.e. 10 points per span. Sensors were mounted at the bottom flange of both external main girders at five different positions: near bearings (beginning and end of the span), ≈ ¼ of the span, mid-span, and ≈ ¾ of the span.

Frequency domain decomposition (FDD) operational modal analysis (OMA) was applied afterwards to extract the modal parameters of the considered span. First and second bending natural frequencies were used for the FEMU.

FINITE ELEMENT MODEL UPDATING (FEMU) OF A VIADUCT

The integration of SHM data with FEMU significantly enhances the value of SHM. The FEMU process involves adjusting the parameters of the FEM based on the measured response data from the SHM system. This iterative process results in a more accurate and reliable model that truly represents the actual structure's behavior.

In this paper, FE model (Figure 3) of the considered span is built in the Abaqus CAE 2016 [14] FE analysis software. It consists of roughly 20.000 C3D20R-type finite elements with an approximate global size of 0.5 m. Updating the FE model was performed by connecting Abaqus to Python 3 [15]. Dimensions and material properties of the FE model were taken from the design documentation [16], [17]. After extensive sensitivity analysis and considering the complex contribution of the safety barriers, directly and indirectly anchored to the edge beam, three variables were updated: Young's modulus adjustment factor of all elements (α_{ALL}), safety barrier "SB1" anchorage reduction factor (φ_{SB1}) and safety barrier "SB2" anchorage reduction factor (φ_{SB2}).

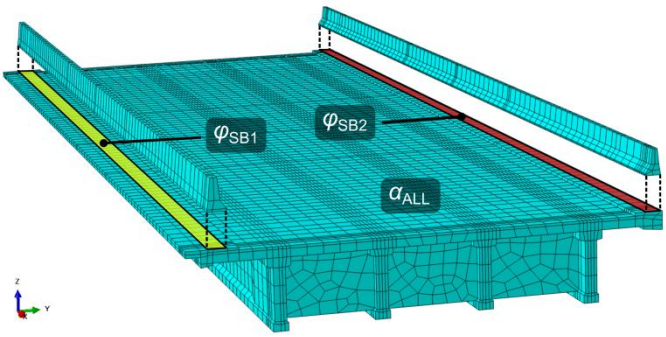

Figure 3. 3D view of the FE model with notations of the updated variables: α_{ALL}, $\varphi_{\mathrm{SB1}}$and φ_{SB2}. Safety barriers are "lifted" on the drawing only to show the location of contact surface for $\varphi_{\mathrm{SB1}}$and φ_{SB2}.

While α_{ALL} is the ratio between updated and design values of Young's modulus of all (8) structural elements, anchorage reduction factors represent the normalized stiffness of the contact between the (partially) anchored safety barriers to the edge beam. The value 0 corresponds to no interaction between safety barriers and the superstructure. In contrast, the value 1 represents the fully connected (anchored) safety barriers.

Strain-based FEMU was performed utilizing the "J_4" type objective function according to [18], a sum of squared differences between modelled and measured strains, normalized to the square of a standard deviation of the measurements. Non-linear optimization utilizes sequential least squares programming (SLSQP) algorithm [19], included in the *scipy* [20] library. The optimum solution was found in 61 steps. Detailed formulation of the objective function as well as properties of the non-linear optimization algorithm can be found in [13].

Acceleration-based FEMU was performed independently from strain-based FEMU. The sum of squared relative differences objective function, i.e. "J_2" type objective function according to [18], was used, where first (B-1) and second (B-2) bending natural frequencies were considered. Particle swarm optimization (PSO) algorithm [21] built in the *pymoo* [22] library was applied with default values of parameters w (0.9), C_1 (2.0) and C_2 (2.0). A population size of 50 individuals was used, and the maximum number of iterations was set to 20.

Results of the FEMU

Results of the strain-based and acceleration-based FEMU are presented in TABLE I and TABLE II, respectively, while TABLE III shows the initial and updated values of α_{ALL}, $\varphi_{\mathrm{SB1}}$and φ_{SB2}.

TABLE I. INITIAL, UPDATED AND MEASURED VALUES OF MAX. STRAINS (STRAIN-BASED FEMU)

Max. strains [μm/m]	Before updating			After updating			Measured		
	V1	V2	V3	V1	V2	V3	V1	V2	V3
SG_01	22.9	34.2	36.6	19.0	28.3	30.3	19.1	29.5	31.5
SG_02	35.3	46.5	48.7	28.3	37.2	39.0	27.1	35.4	37.9
SG_03	36.2	46.8	48.6	28.4	36.6	38.0	27.9	35.5	36.8
SG_04	23.4	34.1	35.9	17.6	25.6	27.0	18.2	27.2	27.4

TABLE II. INITIAL, UPDATED AND MEASURED VALUES OF NATURAL FREQUENCIES (ACCELERATION-BASED FEMU)

Natural frequency [Hz]	Before updating	After updating	Measured
B-1	2.96	3.29	3.32
B-2	9.91	10.76	10.65

TABLE III. INITIAL AND UPDATED VALUES OF α_{ALL}, $\varphi_{\mathrm{SB1}}$and φ_{SB2}

	Strain-based	Acc.-based
Value of the objective function	10.23	0.00017642
α_{ALL} (Young's modulus adjustment factor of all elements)	1.25	1.15
φ_{SB1} (SB1 anchorage reduction factor)	0.00	0.37
φ_{SB2} (SB2 anchorage reduction factor)	0.56	0.43

A noticeable reduction in the deviation between modelled and measured maximum strains can be seen before and after strain-based FEMU. Before FEMU, the absolute deviation was between 16 and 32%, while after, the absolute deviation was between 5 to 6%. For the acceleration-based FEMU, the absolute deviation between 1st and 2nd bending natural frequencies of the initial FE model was 7 and 11%. After FEMU, the deviation dropped to 1 and 1%.

Comparing the final values of α_{ALL}, φ_{SB1} and φ_{SB2} from TABLE III, one can see that acceleration-based FEMU underestimates Young's modulus adjustment factor of all elements (α_{ALL}) and overestimates φ_{SB1} comparing to strain-based FEMU. For the φ_{SB2}, both FEMUs give more comparable results than for φ_{SB1}. From the acceleration-based FEMU it can be concluded that both safety barriers have comparable and non-negligible interaction with the superstructure, which is different from the strain-based FEMU, where safety barrier SB2 has negligible interaction.

While interpreting all three updated variables, one should note that their values are true for the considered load levels and ambient/traffic-induced vibrations and may vary considerably at higher load levels.

CONCLUSIONS

The paper compares updated variables from two types of FEMU: strain-based and acceleration-based. Three variables were updated: Young's modulus adjustment factor of all elements (α_{ALL}) and anchorage reduction factors of both safety barriers (φ_{SB1} and φ_{SB2}). Data for strain-based FEMU is obtained from the strain-gauge sensors installed for the B-WIM.

Strain and acceleration-based FEMU give α_{ALL} values 1.25 and 1.15. Considering a large amount of prestressing tendons in the precast girders, and other reinforcing steel, the value of $\alpha_{\mathrm{ALL}} > 1$ was expected. However, what influences such a deviation between 1.25 and 1.15, needs to be investigated in the future studies.

The interaction between safety barrier 2 and superstructure is non-negligible by both methods. While results of the strain-based FEMU indicate the negligible interaction between safety barrier 1 and superstructure, acceleration-based FEMU indicates this interaction as non-negligible but not greater than for safety barrier 2.

The future aim is to perform acceleration-based FEMU considering more natural frequencies and additional modal parameters (mode shapes and damping), and to perform strain-based FEMU using bridge excitation with random B-WIM weighed vehicles.

ACKNOWLEDGMENT

The authors acknowledge the financial support from the Slovenian Research Agency (Young Researcher funding program (ARRS No. 53694), research core funding No. P2-0260 and P2-0273 and infrastructure program No. I0-0032).

The authors would like to express their gratitude to the Motorway Company of the Republic of Slovenia (DARS d.d.) for permission to use the long-term monitoring results from the considered viaduct. The authors would also like to acknowledge Mr. Jan Kalin and the CESTEL d.o.o. company for their B-WIM-related support.

REFERENCES

1. ASCE Structurally Deficient Bridges | Bridge Infrastructure | ASCE's 2021 Infrastructure Report Card. 2021, 18–25.
2. Forum, I.T. 2021. *ITF Transport Outlook 2021*.
3. Moses, F. 1979. "Weigh-in-Motion System Using Instrumented Bridges,". *J. Transp. Eng., 105*.
4. OBrien, E.J.; Žnidarič, A.; Ojio, T. 2005. "Bridge Weigh-in-Motion – Latest Developments and Applications World Wide," in *Proceedings of the 5th International Conference on Weigh-in-Motion (ICWIM5)*. Jacob, B., OBrien, E.J., OConnor, A., Bouteldja, M. (eds.); LCPC; pp. 39–56., Paris.
5. Žnidarič, A.; Kalin, J.; Kreslin, M. 2017. "Improved Accuracy and Robustness of Bridge Weigh-in-Motion Systems," *Struct. Infrastruct. Eng., 14(4)*.
6. Corbally, R.; Žnidarič, A.; Leahy, C.; Kalin, J.; Hajializadeh, D.; Zupan, E.; Cantero, D. Algorithms for Improved Accuracy of Static Bridge-WIM System, *BridgeMon D1.3 Report*; 2014.
7. Recommendations on the Use of Soft, Diagnostic and Proof Load Testing; European Commission, http://arches.fehrl.org: Brussels, 2009.
8. Wang, H.; Li, A.; Li, J. 2010. "Progressive Finite Element Model Calibration of a Long-Span Suspension Bridge Based on Ambient Vibration and Static Measurements," *Eng. Struct., 32*, 2546–2556, doi:https://doi.org/10.1016/j.engstruct.2010.04.028.
9. Meixedo, A.; Ribeiro, D.; Santos, J.; Calçada, R.; Todd, M. 2021. "Progressive Numerical Model Validation of a Bowstring-Arch Railway Bridge Based on a Structural Health Monitoring System," *J. Civ. Struct. Heal. Monit.* 11, 421–449, doi:10.1007/s13349-020-00461-w.
10. Ereiz, S.; Duvnjak, I.; Fernando Jiménez-Alonso, J. 2022. Structural Finite Element Model Updating Optimization Based on Game Theory. *Mater. Today Proc.* 65:1425–1432, doi:https://doi.org/10.1016/j.matpr.2022.04.401.
11. Žnidarič, A.; Lavrič, I. 2010. "Applications of B-WIM Technology to Bridge Assessment," in *Proceedings of the Fifth International Conference on Bridge Maintenance, Safety and Management IABMAS2010.* Philadelphia, Pennsylvania, USA.
12. Žnidarič, A.; Herga, L.; Pirman, B.; Willenpart, T.; Hevka, P.; Močnik, C.; Ružič, D. 2015. Management of Bridges in Slovenia, National Report.
13. Hekič, D.; Anžlin, A.; Kreslin, M.; Žnidarič, A.; Češarek, P. 2023. "Model Updating Concept Using Bridge Weigh-in-Motion Data. *Sensors*, 23(4), doi:10.3390/s23042067.
14. DS SIMULIA Abaqus 2016 Documentation 2016.
15. Python Software Foundation Python 3.8.16 Documentation Available online: https://docs.python.org/3.8/reference/ (accessed on 31 March 2023).
16. Technical Report about the General Project of the Ravbarkomanda Viaduct (in Slovene); 1970;
17. VA0174 Ravbarkomanda Viaduct Rehabilitation Plan (in Slovene): Notebook 3/1.1-General Part, Technical Part; 2019.
18. Schlune, H.; Plos, M.; Gylltoft, K. 2009. "Improved Bridge Evaluation through Finite Element Model Updating Using Static and Dynamic Measurements," *Eng. Struct., 31:*1477–1485, doi:https://doi.org/10.1016/j.engstruct.2009.02.011.
19. Kraft, D. 1988. "*A Software Package for Sequential Quadratic Programming"*. Weissling.
20. Virtanen, P.; Gommers, R.; Oliphant, T.E.; Haberland, M.; Reddy, T.; Cournapeau, D.; Burovski, E.; Peterson, P.; Weckesser, W.; Bright, J.; et al. 2020. "{SciPy} 1.0: Fundamental Algorithms for Scientific Computing in Python". *Nat. Methods, 17*, 261–272, doi:10.1038/s41592-019-0686-2.
21. Kennedy, J.; Eberhart, R. 1995. "Particle Swarm Optimization" in *Proceedings of the Proceedings of ICNN'95 - International Conference on Neural Networks*, pp. 1942–1948.
22. Blank, J.; Deb, K. Pymoo: Multi-Objective Optimization in Python. *IEEE Access* 2020, *8*, 89497–89509.